

# Effect of chitosan based Al species on coagulation performance and ultrafiltration characteristics under different pH conditions

Wenyu Wang, Qinyan Yue\*, Baoyu Gao, Shuang Zhao, Ruihua Li

Shandong Provincial Key Laboratory of Water Pollution Control and Resource Reuse, School of Environmental Science and Engineering, Shandong University, Jinan 250100, China  
E-mail address: qyyue58@aliyun.com (Q. Yue).

## Abstract

In this study, the tendency of coagulation performances, floc characteristics and membrane resistances under different pH conditions in coagulation–ultrafiltration hybrid process (C-UF) was investigated by different Al species and chitosan (CS). Results indicated that CS as coagulation aid was independent of aluminum species. Coagulation efficiencies of three Al species ( $Al_a$ ,  $Al_b$  and  $Al_c$ ) combined with CS were enhanced comparing with Al species used alone and showed similar variation tendencies during the pH range. The values of floc size and strength/recovery factor were relatively high at pH 6 in coagulation process, and the maximum fractal dimension was achieved under alkaline conditions generally due to adsorption sweeping effect of aluminum hydrolysates.  $Al_a/Al_b/Al_c$  combined with CS contributed to larger flocs, higher recovery factors and smaller fractal dimension values than those without CS. The results of ultrafiltration experiments showed that membrane resistances during alkaline ranges were higher than those of acidic conditions in C-UF, which indicated membrane fouling was more serious in alkaline range. In addition, the total membrane resistance was decreased significantly due to CS addition.

## Keywords:

pH, Al species, Chitosan, Floc characteristics, Membrane resistances

## INTRODUCTION

In water treatment process, many types of coagulants have been widely used, especially aluminum salt coagulants. As aluminum salt dosed into water, there would be a series of hydrolysis reactions and different Al species were generated:  $Al_a$ ,  $Al_b$ , and  $Al_c$  (Duan & Gregory 2003). Previous study has shown that  $Al_a$  has better removal efficiency of natural organic matter (NOM) under certain conditions (Yan *et al.* 2007), since the hydrolysate species were unstable and hard to control as a small fluctuation of conditions, such as pH, temperature, etc (Golob *et al.* 2005; Sher *et al.* 2013). It has been demonstrated that the amount of electric charges for hydrolyzed Al was determined by the solution pH, thus pH is a crucial way to control the hydrolysis species of Al salt. The NOM removal efficiency of coagulants is usually not perfect and some of which are harmful to environment (Lee *et al.* 2011). In order to improve the NOM removal efficiency, it is indispensable to find high efficient and non-toxic coagulant aids. As a kind of bio-coagulant, chitosan (CS) was the second most abundant biopolymer after cellulose in the world which produced by the deacetylation of chitin (Renault *et al.* 2009). In the process of coagulation, CS which is described as a cationic polyelectrolyte is easy to exposure to protons by hydrolysis, and then the micro particles combine to settle down mutually. These novel three Al species combined with CS was better than their individual components, which lead to enhanced coagulant stability and wider effective pH range than that of Al salts coagulants. In this paper, the combination of Al species with CS was short for  $Al_a/Al_b/Al_c$ -CS.

Recently, the removal of turbidity and NOM from water is a problem for producing potable water, of which coagulation are considered to be the most common process. In coagulation process, adjustment of pH is a significant way to enhance turbidity and NOM removal efficiency. Ultrafiltration (UF) which has been widely used is not effective to remove NOM, however membrane fouling is an important issue and face with enormous challenges in the UF process. In general, to improve the efficiency removal of NOM and alleviate membrane fouling, combination of coagulation and UF (C-UF) is necessary. As previous research (Choo *et al.* 2007), in C-UF process the performance was closely related to coagulant type, coagulation condition and resultant

floc characteristics which were strongly affected by pH. Thus, the coagulation performance, floc characteristics and membrane fouling under different pH conditions by three Al species as coagulant and CS as coagulant aid in C-UF process should be further researched.

In this study, the coagulation performance of  $Al_a/Al_b/Al_c$ -CS and  $Al_a/Al_b/Al_c$  were compared to demonstrate its flocculating efficiency. The effect of solution pH on floc properties (strength factor, recovery factor and fractal dimension) were comparatively studied. Membrane resistances under different pH conditions were used to measure the degree of membrane fouling. In general, coagulation models of three Al species combined with CS under different pH conditions were described to further research the mechanisms in HA-Kaolin treatment, and a detailed investigation on coagulation efficiency, floc characteristic and membrane fouling mechanism was discussed.

## **MATERIALS AND METHODS**

### **Coagulants**

Three different Al species were used as coagulant and CS was selected as coagulant aid. The procedures of coagulants preparation were listed as follows:  $Al_a$  solution was prepared by directly dissolving  $AlCl_3 \cdot 6H_2O$  in deionized water. The synthesis method of  $Al_b$ , NaOH was added into  $AlCl_3 \cdot 6H_2O$  solution with the B value ( $[OH^-]/[Al^{3+}]$  mole ratio) of 2.4, and then purify with ethanol-acetone solution (Zhao *et al.* 2011). The method of  $Al_c$  is similar to that of  $Al_b$  but the reaction temperature is much higher, and the process of purification uses methanol/acetone solution.

CS solution was prepared by dissolving in 1% w/w HCl, and the mixture was stirred until no sediment existed, and then diluted with deionized water to 50 mL.

### **Water samples**

Humic acid (HA) was the main material in natural organic matter. In addition, Kaolin was used to simulate the raw water. Thus, the water sample was prepared by HA and kaolin, which was based on previous methods. The water sample was prepared by using tap water to make its concentration of 10 mg HA/L, and the physicochemical parameters were listed as follows: Turbidity =  $15.0 \pm 0.5$  NTU,  $UV_{254}$  absorbance =  $0.305 \pm 0.010 \text{ cm}^{-1}$ , Dissolved Organic Carbon =  $5.350 \pm 0.200$  mg/L, Zeta potential =  $-20.0 \pm 0.7$  mV, pH =  $8.10 \pm 0.05$ .

### **Jar tests**

Coagulation experiments were operated by using a programmatic jar-test apparatus (Zhongrun Water Industry Technology Development Co., Ltd., China) to confirm the effect of pH on coagulation performance, and predetermined pH values (from 4 to 9) of samples were adjusted by 1.0 mol/L HCl and NaOH solutions. In the first place, amount of Al species coagulants were added into water samples during the rapid stirring (200 rpm), then CS was dosed with a 30 s interval. After that each sample continued rapid stirring for 1 min, followed by slow mixing (40 rpm) for 15 min and quiescent settling for 30 min. To determine coagulation performance, after sedimentation process about 200 mL samples were taken for turbidity and zeta potential measurement (Zetasizer Nano ZS, Malvern, UK). The remaining samples were filtered by 0.45  $\mu\text{m}$  fiber for  $UV_{254}$  measurement (Precision Scientific Instrument Co., Ltd., China) and DOC analysis (TOC-VCPH, Shimadzu, Japan).

### **Floc properties**

Dynamic floc sizes were monitored by Mastersizer 2000 (Malvern, UK). These experiments were conducted on the jar tester and the procedure was similar to coagulation experiment which without sedimentation. The suspended floc was monitored by a peristaltic pump (LEAD-1, Longer Precision

Pump, China) which was placed in the downstream of Mastersizer to prevent flocs broken before measurement. During the process of coagulation, the median volumetric diameter ( $d_{50}$ ) which reflects floc size was measured every 30 s, and then the data were recorded automatically by computer.

The floc properties were described by strength factor ( $S_f$ ), recovery factor ( $R_f$ ) and fractal dimension ( $D_f$ ).  $D_f$  which describe flocs structure was related to the scattered light intensity ( $I$ ) and scattering vector ( $Q$ ). They were calculated as follows (Wu *et al.* 2002; Gonzalez-Torres *et al.* 2014):

$$S_f = d_2/d_1 \times 100 \quad (1)$$

$$R_f = (d_3 - d_2)/(d_1 - d_2) \times 100 \quad (2)$$

$$I \propto Q^{-D_f} \quad (3)$$

In these equations,  $d_1$  is the average floc size in firstly steady period,  $d_2$  is the floc size for the last point at breakage phase and  $d_3$  is the floc size after regrowth to a steady region. In addition,  $D_f$  values can be calculated by the slope of a diagram of  $I$  and  $Q$  on a log-log scale.

### Membrane fouling experiments

Ultrafiltration experiments were conducted using a 300 mL dead-end stirred batch after coagulation (without sedimentation). A constant trans-membrane pressure (TMP) was provided at 80 kPa by nitrogen gas. UF membranes (PLHK07610, Millipore, USA) were used with molecular weight cutoff of 100 kDa and filter diameter of 76 mm. The mass of infiltration was monitored by an electronic balance (MSU5201S-000-D0, SartoriusAG, Germany), which was connected to computer. Membrane resistances could intuitively reflect the membrane fouling. In general, the total hydraulic resistance ( $R_t$ ) consisted of external fouling ( $R_{ef}$ ) and internal fouling ( $R_{if}$ ). Among them,  $R_{ef}$  contains loosely-attached resistance ( $R_{ef-l}$ ) and strongly-attached resistance ( $R_{ef-s}$ ), and  $R_{if}$  includes reversible resistance ( $R_{if-r}$ ) and physically irreversible fouling resistance ( $R_{irr}$ ) (Lin *et al.* 2015).

The experiments were carried as follows: (1) 100 mL deionized water was carried out to obtain flux  $J_0$ ; (2) 1 L water sample which after the process of pre-coagulated was ultra-filtrate to get  $J_1$ ; (3) deionized water was added with the stirring rate of 200 rpm to obtain flux  $J_2$ ; (4) the membrane was taken out and wiped to remove the strongly-attached cake layer, and then deionized water was carried out at low stirring speed to get  $J_3$ ; (5) the reverse side of the membrane was upwards with filtration of 100 mL deionized water, and followed by filtering deionized water to obtain  $J_4$  (Li *et al.* 2014). According to the experiments above, the  $R_m$ ,  $R_{ef-l}$ ,  $R_{ef-s}$ ,  $R_{if-r}$  and  $R_{irr}$  can be calculated as follows:

$$R_m = TMP/(\mu J_0) \quad (8)$$

$$R_{ef-l} = TMP/(\mu J_1) - TMP/(\mu J_2) \quad (9)$$

$$R_{ef-s} = TMP/(\mu J_2) - TMP/(\mu J_3) \quad (10)$$

$$R_{if-r} = TMP/(\mu J_3) - TMP/(\mu J_4) \quad (11)$$

$$R_{irr} = TMP/(\mu J_4) - TMP/(\mu J_0) \quad (12)$$

where  $R_m$ , TMP and  $\mu$  are clean membrane resistance ( $m^{-1}$ ), trans- membrane pressure (Pa) and dynamic viscosity of the feed water (Pa s), respectively.

## RESULTS AND DISCUSSION

### Effect of pH on HA removal

Initially, standardized coagulation jar tests were performed to ascertain the optimum dosage of Al

species and CS. The HA and turbidity removal efficiencies under different pH conditions were studied respectively. Our previous study indicated that the efficiencies removal of UV<sub>254</sub> and DOC were best at Al dosage of 4 mg/L and CS dosage of 1 mg/L. Therefore, in this study 4 mg/L of Al and 1 mg/L of CS dosage were chosen to conduct the following experiments.

As showed in Fig. 1a, the trends of residual turbidity with pH were similar. The residual turbidity of Al species used alone changed more significantly than that of CS used, which indicated that CS added generated larger flocs which easier sediment as pH values varied from 4 to 9. In acidic range Al<sub>c</sub> may be hydrolyzed into Al<sub>b</sub> and then improved the efficiency of coagulation, on the contrary Al<sub>a</sub> was not easier to hydrolyze, but Al<sub>a</sub> molecules were easier to get together and form bigger flocs under alkaline conditions, so for three coagulants the minimum residual turbidity was Al<sub>c</sub>/Al<sub>c</sub>-CS under acidic conditions and that of Al<sub>a</sub>/Al<sub>a</sub>-CS under alkaline region. The minimum residual turbidity for coagulants was achieved at pH 6 except Al<sub>b</sub>/Al<sub>b</sub>-CS, which mainly attribute to the effect of pH for Al<sub>b</sub> could be limited during coagulation process.

The removal efficiencies of UV<sub>254</sub> and DOC increased significantly first, until they reached the maximum value at pH 6 and then decreased sharply in Fig. 1b and 1c. The removal efficiencies of UV<sub>254</sub> and DOC were promoted when CS added, due to the mechanism of CS was charge neutralization (Ng *et al.* 2012) which could form compression of the electric double layer. The pH values had more crucial for Al<sub>a</sub> species than that of Al<sub>b</sub> and Al<sub>c</sub> under acidic conditions. This phenomenon because the coagulation mechanism of Al<sub>a</sub> mainly was hydrolysis action which significantly affected by the pH, but for Al<sub>b</sub> and Al<sub>c</sub> which were the pre-hydrolysis products of Al<sub>a</sub> had less impact on the pH about hydrolysis action. In addition, HA molecules became more hydrophobic and its combination would close to the isoelectric point at pH 6. But in alkaline range, the electrostatic repulsion became more significant led to low removal efficiency.

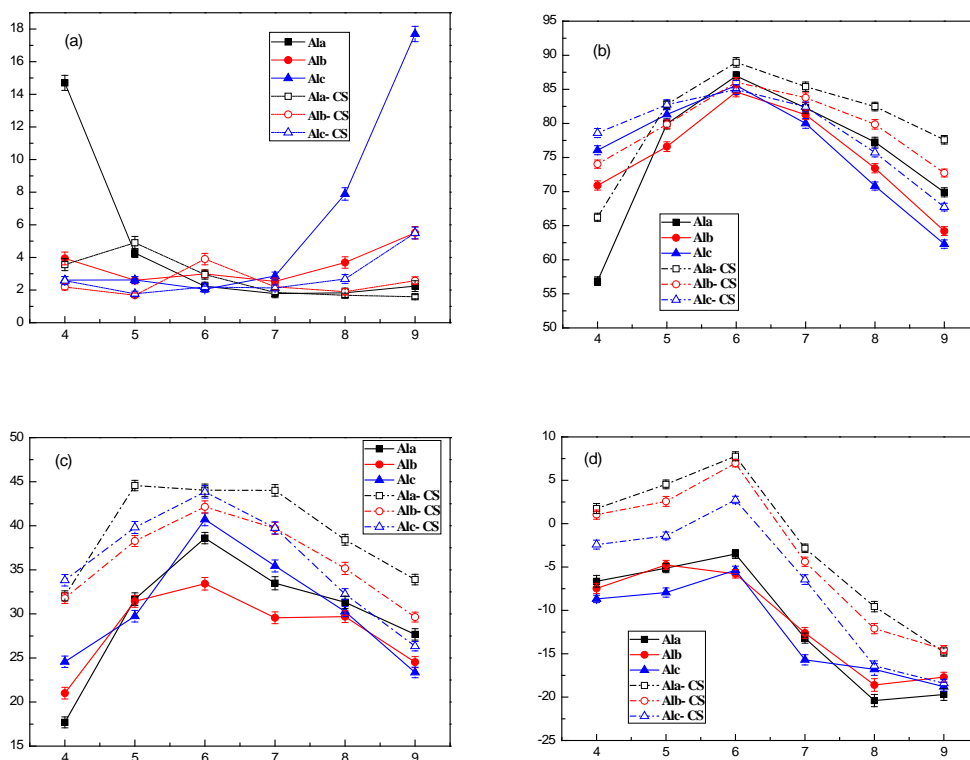


Figure 1 Coagulation efficiency of different Al species as coagulant and CS as coagulant aid under different pH conditions: (a) residual turbidity, (b) UV<sub>254</sub> removal efficiency, (c) DOC removal efficiency, (d) zeta potential.

Fig. 1d showed the variation of zeta potential under various pH values. In all the cases, zeta potential increased gently when pH reached 6, and then decreased sharply as pH further increased, which was consistent with the trends of UV<sub>254</sub> and DOC removal. This indicated that charge neutralization was main mechanism in acid ranges, but coagulants removed HA particles mainly through absorption bridging and sweeping when pH exceed 7. In acidic ranges, major hydrolyzed Al species ( $\text{Al}^{3+}$ ,  $\text{Al}(\text{OH})^{2+}$  and  $\text{Al}(\text{OH})_2^+$ ) were positively charged monomer ions. Polymeric positive species were produced and combined with negative particles to form co-precipitates as pH increased to neutral. Al species transformed into  $\text{Al}(\text{OH})_3$  and  $\text{Al}(\text{OH})_4^-$  under alkaline conditions (Gregor *et al.* 1997). Fig. 2 indicated that the mechanisms of HA removal for different Al species as coagulant and CS as coagulant aid at pH 6. Functional group of Al species adsorbed numerous colloidal particles, and formed micro flocs and then reacted with CS by charge neutralization and absorption bridging during mixing, so zeta potential increased significantly when CS added.

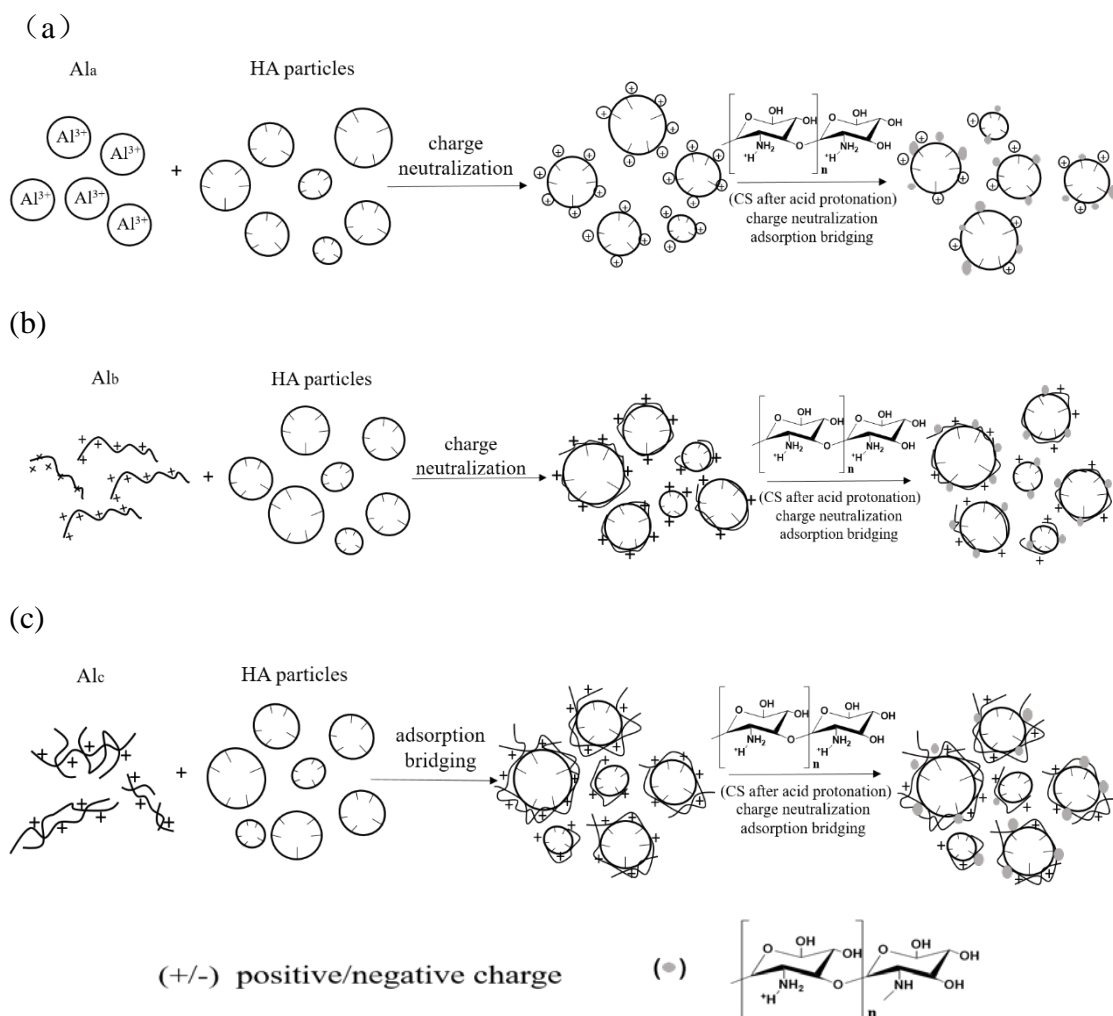


Figure 2 Mechanisms of HA removal by different Al species as coagulant and CS as coagulant aid at pH 6: (a) Al<sub>a</sub>, (b) Al<sub>b</sub>, (c) Al<sub>c</sub>.

## Flocs properties

### Floc size

Floc sizes under different pH conditions were showed in Fig. 3. This indicated that pH had significant influence on floc size. This could be explained that products by Al salt hydrolyzation

with positively charged were quickly neutralized negatively charged particles to form primary flocs during coagulation, and then these primary flocs with small sizes absorbed HA macromolecules to grow. At the same time, large flocs would be broken by collision in the process of aggregation, and a balance plateau of flocs size was achieved when the velocities of aggregate and breakage were equal.

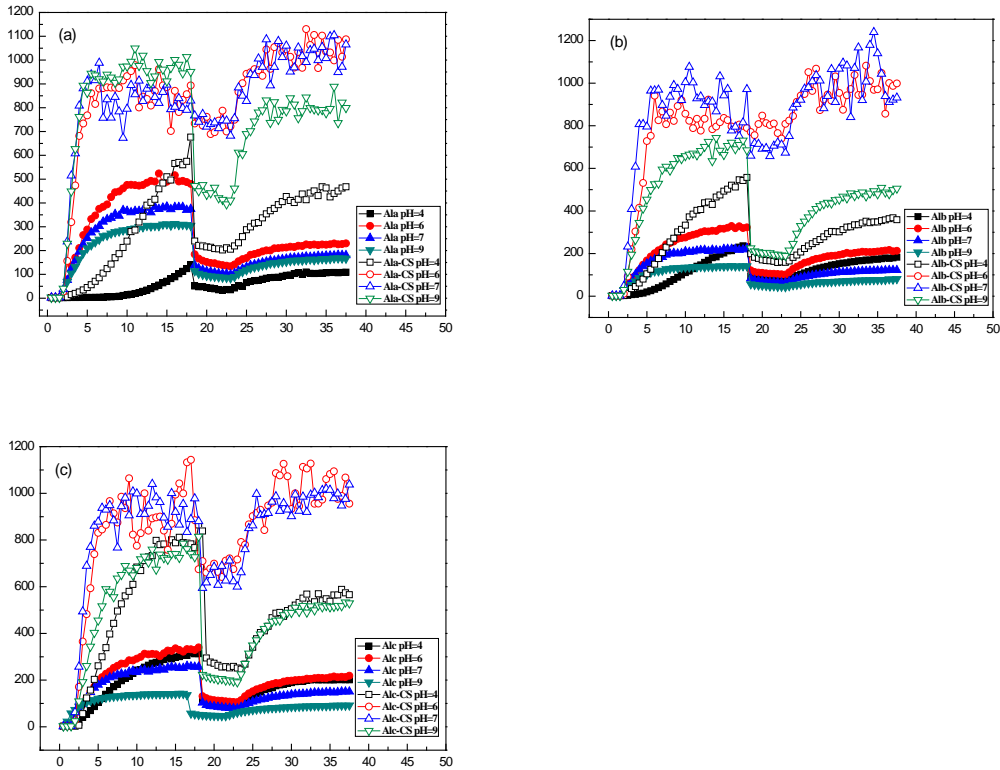


Figure 3 The trend of floc size under different pH conditions: (a)  $Al_a$ , (b)  $Al_b$ , (c)  $Al_c$ .

Under the same dosage and pH conditions, floc sizes by different Al coagulants were in the following order:  $Al_a > Al_c > Al_b$ , which was due to the mechanisms of different Al species.  $Al_a$  which rapidly hydrolyzed to  $Al_b$  reacted with HA and kaolin particles to form larger flocs under this pH range. Previous research suggested that  $Al_b$  which was metastable to dilution or to changes as pH changes was converted slowly (Lin *et al.* 2008), so the floc sizes of  $Al_b$  was smaller. The mechanism of  $Al_c$  was sweeping and bridging as showed in Fig. 2 which could generate larger flocs, because the floc particles formed by charge neutralization were smaller than those formed by sweeping and bridging (Zhao *et al.* 2011). But when CS used, the floc size of  $Al_c$ -CS had larger size in acid ranges and  $Al_a$ -CS had greater advantages under alkaline conditions.

Under acidic conditions, sweeping was the main mechanism when Al species were dosed firstly due to electrostatic repulsion, and then CS attached to flocs surface and combined other micro flocs because of adsorption bridging. Thus, the floc size tendency of  $Al_c$ -CS was the most significant. Floc size achieved maximum value at pH 6 when Al species coagulants used alone, because HA was less hydrophilic and easier to destabilize and precipitate. But when CS added, floc size became larger caused by charge neutralization, which achieved about 900  $\mu m$ . Under alkaline conditions, the main mechanisms of charge neutralization caused by negatively charged of main parts and positively charged CS to form co-precipitation by charge neutralization. Therefore, the floc size of  $Al_a$ -CS had greater advantages in alkaline ranges.

### Floc strength and structure

Floc strength and recovery ability as the variation of pH were illustrated in Table 1. In general, maximum  $S_f$  and  $R_f$  were mainly acquired at pH 6 due to the strongest charge neutralization effect. The smaller floc size usually had larger  $S_f$ , which might because small flocs would have strong ability to resist shear (Jarvis *et al.* 2005b). These demonstrated that  $S_f$  by different Al coagulants were in the following order:  $Al_b > Al_c > Al_a$ . Most of  $S_f$  was increased with CS added especially in partial neutral circumstance, which was caused by the strongest charge neutralization. Moreover, the larger floc size also had bigger  $R_f$  (Jarvis *et al.* 2005a). The reason was that flocs concentrations were increased and combine with each other to form big ones in the process of collisions. As a consequence, the order of  $R_f$  was contrary to  $S_f$  for different Al coagulants.  $R_f$  was significantly increased when CS added in neutral and alkaline circumstance due to charge neutralization. But under acidic conditions, CS with positively charged could generate electrostatic repulsion, leading to lower  $R_f$ .

Table 1 Floc strength and recovery factors under different pH conditions.

Parameter	Coagulant	pH			
		4	6	7	9
Strength factor ( $S_f$ )	$Al_a$	25.14±0.22	27.88±0.35	26.68±0.33	27.55±0.27
	$Al_a$ -CS	30.41±0.27	80.81±0.52	62.20±0.47	23.21±0.25
	$Al_b$	32.70±0.31	33.41±0.41	30.52±0.36	31.10±0.29
	$Al_b$ -CS	29.48±0.29	92.54±0.57	69.29±0.45	27.57±0.23
	$Al_c$	30.01±0.33	31.12±0.39	28.55±0.28	30.31±0.25
	$Al_c$ -CS	28.10±0.18	80.98±0.54	68.15±0.39	33.46±0.31
Recovery factor ( $R_f$ )	$Al_a$	70.33±0.51	67.75±0.45	49.35±0.32	57.40±0.41
	$Al_a$ -CS	55.71±0.47	213.13±0.97	259.35±1.09	71.95±0.45
	$Al_b$	67.75±0.54	50.34±0.39	35.66±0.28	49.12±0.38
	$Al_b$ -CS	50.21±0.42	133.99±0.75	86.61±0.54	63.71±0.49
	$Al_c$	48.89±0.39	48.26±0.35	40.52±0.34	50.52±0.35
	$Al_c$ -CS	57.26±0.48	142.09±0.72	155.88±0.77	54.26±0.39

Fig. 4 showed the variations of  $D_f$  with time under different initial pH conditions. As can be seen,  $D_f$  was stable at the growth period and regrowth period, but during breakage period it increased rapidly. These phenomenon could be explained that floc size would decrease rapidly when gave a high shear stress, and formation of micro flocs which had denser structure as well as larger  $D_f$  values. In addition, more compact flocs which had more stable structure would be reformed after the breakage period. These caused  $D_f$  at regrowth period was much larger than that of growth period. Previous studies demonstrated that flocs formed in sweeping were more compact than that of other mechanisms (Li *et al.* 2006). Therefore,  $D_f$  value of  $Al_c$  was larger than that of  $Al_a$  and  $Al_b$ .

In general, carboxyl groups of HA could release carboxylic which were exposed to cationic coagulant at higher pH, leading to the  $D_f$  values in alkaline range were larger than that in acidic range.  $D_f$  showed a reduction when CS as coagulation aid was added, which was related to relatively large floc formed by the same effect usually had a looser structure. These were consistent with previous researches which compact structure had larger fractal dimension (Jarvis *et al.* 2005a).



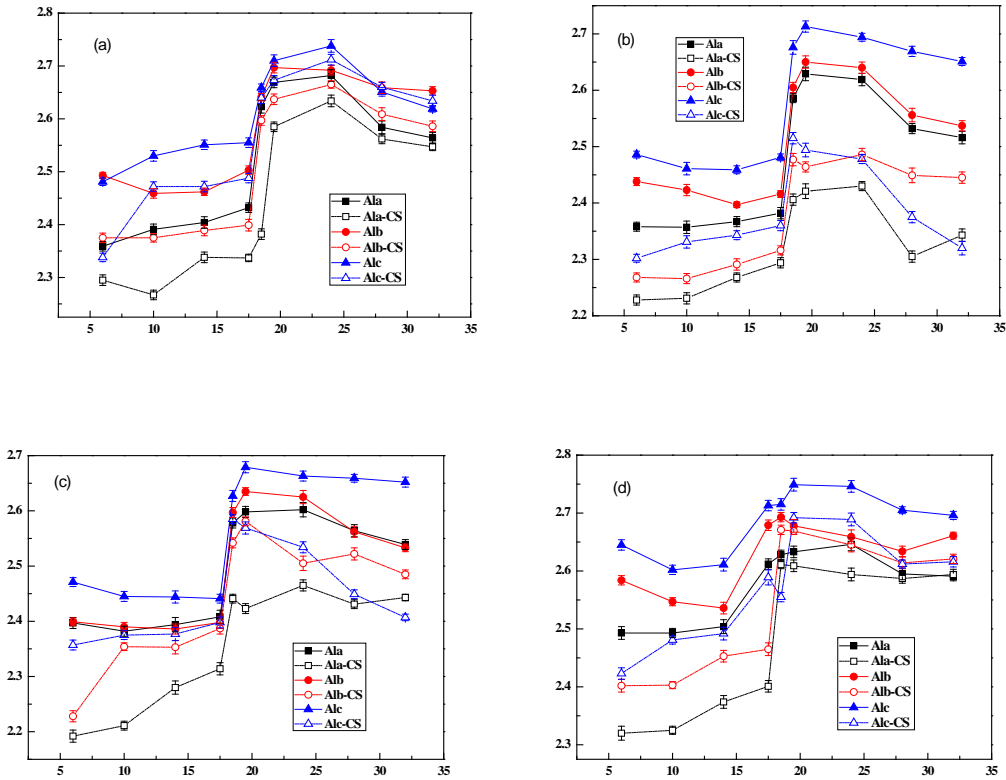


Figure 4 Fractal dimension under different pH conditions: (a) pH 4, (b) pH 6, (c) pH 7, (d) pH 9.

### Membrane resistances

The results of  $R_{ef-l}$ ,  $R_{ef-s}$ ,  $R_{if-r}$  and  $R_{irr}$  under different pH conditions were showed in Fig. 5. The slightest membrane flux with smallest total resistances occurred at pH 6, but the maximum value of total resistances became the most serious membrane fouling at pH 9. Addition of CS resulted in the reduction of the total membrane resistance, which in the following order:  $Al_a/Al_b/Al_c-CS < Al_a/Al_b/Al_c$ . This demonstrated that the resistances of membrane were associated with floc sizes and fractal dimension.

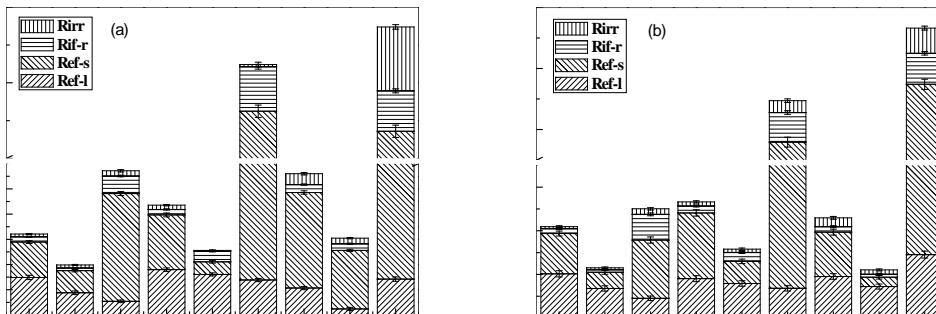


Figure 5 Resistances on membrane fouling in ultrafiltration process under different pH conditions: (a)  $Al_a/Al_b/Al_c$ , (b)  $Al_a/Al_b/Al_c-CS$ .

The external resistances include  $R_{ef-l}$  and  $R_{ef-s}$ , of which  $R_{ef-l}$  was loosely attached external fouling and could be removed by stirring. But the denser flocs would not easier to be broken by stirring at rate of 200 rpm. Fig. 5 showed that floc fractal structure mainly contributed to influence on  $R_{ef-l}$ .



The  $R_{ef-1}$  value of  $Al_a$  and  $Al_b$  was smaller under alkaline conditions, because flocs seemed to be more porous and looser (Guigui *et al.* 2002).  $Al(OH)_4^-$  which the crucial form hydrolyzed by  $Al_c$  carried negative electricity layer, and it could not generate larger particles at pH 9, which resulted in larger  $R_{ef-1}$ . Fig. 4 showed that  $D_f$  of flocs were decreased when CS dosed with looser cake layers, and large floc sizes generated at the same pH ranges. These have positive effect for  $R_{ef-1}$ , and led to the resistance decreased with CS added.

In UF process,  $R_{ef-s}$  which was strongly attached membrane could not be removed by stirring. The previous research indicated that larger floc sizes always generated lower fouling resistance (Wang *et al.* 2008). Larger  $D_f$  with denser aggregate which always generated larger fouling resistance, and flocs not easy to break into micro particles under rapid stirring hydraulic conditions (Lee *et al.* 2011), and most of them could be wiped to remove. Therefore,  $R_{ef-s}$  was larger under alkaline conditions, on the other hand  $Al_c$  caused greater fouling resistance. The significantly reduction of  $R_{ef-s}$  with CS was observed, because the floc sizes were much larger than that of UF processes without CS dosed during the same pH ranges.

Internal membrane resistance ( $R_{if-r}$  and  $R_{irr}$ ) was generated by particles and micro flocs with molecule weight (MW) smaller than 100 kDa. These flocs could not be rejected onto membrane surface and attach inside the membrane pores. The pores fouling could be removed by backwash caused the resistance of reversible (Li *et al.* 2014).  $R_{if-r}$  raised with increasing pH, these because large amount of  $OH^-$  in alkaline solution neutralized the positive charges of coagulations, and then reducing neutralization of coagulation surface ions with a negative charge of HA. But  $R_{if-r}$  decreased when CS was added, and these were in accordance with Fig. 4.

$R_{irr}$  as another inner membrane resistance caused long-term fouling of membrane pores, which could significantly impact the membrane durability. These fouling could not be removed by backwash, lead to the increase of  $R_{irr}$ . Larger  $R_{irr}$  was generated under alkaline solution caused by the influence of floc fractal structure, which was similar to  $R_{if-r}$ . Fig. 1 showed that the  $UV_{254}$  and DOC removal was reduced with CS added, thus  $R_{irr}$  was less than that without CS. These phenomena demonstrated that even external resistances and internal resistances seem to be similar, and the flocs characters as well as the removal of organic matter would determine the difficulty degree for membrane fouling, which was important for maintenance of long range UF operation.

## CONCLUSIONS

The results of this paper demonstrated that the variation of pH significant impact on coagulation efficiency, floc characteristic and membrane filtration in C-UF. HA removal efficiency was higher at pH 6, and  $Al_a/Al_b/Al_c$ -CS increased the removal ratios compared with  $Al_a/Al_b/Al_c$ . Flocs under acidic conditions were smaller than these under alkaline conditions except for  $Al_c$ . Moreover, larger and looser flocs were formed when CS dosed. Membrane resistances were related to membrane fouling which in acidic ranges was less serious than that in alkaline ranges, furthermore the membrane fouling was the lowest at pH 6.

## ACKNOWLEDGEMENTS

This study was supported by the National Natural Science Foundation of China (No. 21377071) and Tai Shan Scholar Foundation (No. ts201511003). The kind suggestions from the anonymous reviewers are greatly acknowledged.

## REFERENCES

- Choo K.-H., Choi S.-J. and Hwang E.-D. (2007). Effect of coagulant types on textile wastewater reclamation in a combined coagulation/ultrafiltration system. *Desalination* **202**, 262–70.
- Duan J. and Gregory J. (2003). Coagulation by hydrolysing metal salts. *Advances in Colloid and Interface Science* **100-102**, 475-502.
- Golob V., Vinder A. and Simonic M. (2005). Efficiency of the coagulation/flocculation method for the treatment of dyebath effluents. *Dyes and Pigments* **67**(2), 93-7.
- Gonzalez-Torres A., Putnam J., Jefferson B., Stuetz R. M. and Henderson R. K. (2014). Examination of the physical properties of *Microcystis aeruginosa* flocs produced on coagulation with metal salts. *Water Res* **60**, 197-209.
- Gregor J. E., Nokes C. J. and Fenton E. (1997). Optimising natural organic matter removal from low turbidity waters by controlled pH adjustment of aluminium coagulation. *Water Res* **31**(12), 2949–58.
- Guigui C., Roucha J. C., Durand-Bourlier L., Bonnelyeb V. and Aptel P. (2002). Impact of coagulation conditions on the in-line coagulation/UF process for drinking water production *Desalination* **147**, 95-100.
- Jarvis P., Jefferson B., Gregory J. and Parsons S. A. (2005a). A review of floc strength and breakage. *Water Res* **39**(14), 3121-37.
- Jarvis P., Jefferson B. and Parsons S. A. (2005b). Breakage, Regrowth, and Fractal Nature of Natural Organic Matter Flocs. *Environmental Science & Technology* **39**(7), 2307-14.
- Lee K. E., Teng T. T., Morad N., Poh B. T. and Mahalingam M. (2011). Flocculation activity of novel ferric chloride–polyacrylamide (FeCl<sub>3</sub>-PAM) hybrid polymer. *Desalination* **266**(1-3), 108-13.
- Li K., Liang H., Qu F., Shao S., Yu H., Han Z.-s., Du X. and Li G. (2014). Control of natural organic matter fouling of ultrafiltration membrane by adsorption pretreatment: Comparison of mesoporous adsorbent resin and powdered activated carbon. *Journal of Membrane Science* **471**, 94-102.
- Li T., Zhu Z., Wang D., Yao C. and Tang H. (2006). Characterization of floc size, strength and structure under various coagulation mechanisms. *Powder Technology* **168**(2), 104-10.
- Lin J. L., Chin C. J., Huang C., Pan J. R. and Wang D. (2008). Coagulation behavior of Al(13) aggregates. *Water Res* **42**(16), 4281-90.
- Lin T., Lu Z. and Chen W. (2015). Interaction mechanisms of humic acid combined with calcium ions on membrane fouling at different conditions in an ultrafiltration system. *Desalination* **357**, 26-35.
- Ng M., Liana A. E., Liu S., Lim M., Chow C. W., Wang D., Drikas M. and Amal R. (2012). Preparation and characterisation of new-polyaluminum chloride-chitosan composite coagulant. *Water Res* **46**(15), 4614-20.
- Renault F., Sancey B., Badot P. M. and Crini G. (2009). Chitosan for coagulation/flocculation processes – An eco-friendly approach. *European Polymer Journal* **45**(5), 1337-48.
- Sher F., Malik A. and Liu H. (2013). Industrial polymer effluent treatment by chemical coagulation and flocculation. *Journal of Environmental Chemical Engineering* **1**(4), 684-9.
- Wang J., Guan J., Santiwong S. R. and Waite T. D. (2008). Characterization of floc size and structure under different monomer and polymer coagulants on microfiltration membrane fouling. *Journal of Membrane Science* **321**(2), 132-8.
- Wu R. M., Lee D. J., Waite T. D. and Guan J. (2002). Multilevel structure of sludge flocs. *J Colloid Interface Sci* **252**(2), 383-92.
- Yan M., Wang D., Qu J., He W. and Chow C. W. (2007). Relative importance of hydrolyzed Al(III) species (Al(a), Al(b), and Al(c)) during coagulation with polyaluminum chloride: a case study with the typical micro-polluted source waters. *J Colloid Interface Sci* **316**(2), 482-9.
- Zhao H.-Z., Wang H.-Y., Dockko S. and Zhang Y. (2011). The formation mechanism of Al<sub>13</sub> and its purification with an ethanol–acetone fractional precipitation method. *Separation and Purification Technology* **81**(3), 466-71.